Systematic study on *α*-decay half-lives of uranium isotopes with a screened electrostatic barrier*

Yang-Yang Xu(徐杨洋)[1]   De-Xing Zhu(祝德星)[1]   You-Tian Zou(邹有甜)[1†]   Xi-Jun Wu(吴喜军)[2‡]

Biao He(何彪)[3]   Xiao-Hua Li(李小华)[1,4,5,6§]

[1]School of Nuclear Science and Technology, University of South China, Hengyang 421001, China
[2]School of Math and Physics, University of South China, Hengyang 421001, China
[3]College of Physics and Electronics, Central South University, Changsha 410083, China
[4]National Exemplary Base for International Sci & Tech. Collaboration of Nuclear Energy and Nuclear Safety, University of South China, Hengyang 421001, China
[5]Cooperative Innovation Center for Nuclear Fuel Cycle Technology & Equipment, University of South China, Hengyang 421001, China
[6]Key Laboratory of Low Dimensional Quantum Structures and Quantum Control, Hunan Normal University, Changsha 410081, China

Abstract: In the present work, we systematically study the *α*-decay half-lives of uranium (*Z*=92) isotopes based on the Gamow model with a screened electrostatic barrier. There are only two adjustable parameters in our model i.e. the parameter g and the screening parameter t in the Hulthen potential for considering the screened electrostatic effect of the Coulomb potential. The calculated results are in good agreement with experimental data, and the corresponding root-mean-square (rms) deviations of uranium isotopes with *α* transition orbital angular momentum l=0 and l=2 are 0.141 and 0.340, respectively. Moreover, we extend this model to predict *α*-decay half-lives of uranium isotopes whose *α* decay is energetically allowed or observed but not yet quantified in NUBASE2020. For comparison, the modified Hatsukawa formula (XLZ), the unified Royer formula (DZR), the universal decay law (UDL) and the Viola−Seaborg−Sobiczewski formula (VSS) are also used. The predictions are basically consistent with each other. Meanwhile, the results also indicate that *N*=126 shell closure is still robust at *Z*=92 and the spectroscopic factor S_α is almost the same for uranium isotopes with the same l.

I. INTRODUCTION

α decay has always been a hot topic in nuclear physics because it can provide abundant nuclear structure information such as ground state [1], nuclear shell effect [2], energy levels [3], nuclear shape coexistence [4–6], low lying states [7] and so on. As one of the most important decay modes of superheavy nuclei [8], *α* decay was first explained by Rutherford in 1908 in terms of a process where a parent nucleus emits a ^{4}He particle [9]. Following the foundation and development of quantum mechanics, Gamow [10] and Condon and Gurney [11] in 1928 intepreted the theory of *α* decay as a quantum penetration of *α* particles via tunneling.

Up to now, based on Gamow theory, a great deal of models and/or approaches have been put forward to study *α* decay. The commonly used models are the cluster model [12–18], the Coulomb and proximity potential model (CPPM) [19, 20], the two-potential approach (TPA) [21–27], the density dependent M3Y (DDM3Y) effective interaction [28–33], the shell model [34], the generalized liquid drop model (GLDM) [35–37], the fission-like model [38–40] and so on. These models, with their own merits and failures, have been in acceptable agreement with experimental data. Moreover, there are lots of efficient and useful empirical formulas to calculate the *α*-decay half-lives such as the Viola−Seaborg formula (VS)

[41], the universal decay law (UDL) [42, 43], the Royer formula [44], the Hatsukawa formula [45] and Qian *et al.* formula (YQZR) [46, 47] while their improvements are the Viola–Seaborg–Sobiczewski formula (VSS) [48] and the modified Viola –Seaborg formula (MVS) [49], the modified universal decay law (MUDL) [50], the unitary Royer formula (DZR) [51], the modified Hatsukawa formula (XLZ) [52] and the modified Yibin *et al.* formula (MYQZR) [53], respectively. From the experimental aspect, the development of radioactive beams and low temperature detector technology make it possible to synthesize new superheavy nuclei [54] and search new α-emitters in artificially occurring nuclides [55, 56].

Recently, we were intrigued by a series of reports on the synthesis of uranium isotopes. In 2015, the new neutron-deficient isotope ^{215}U was produced in the complete-fusion reaction ^{180}W(^{40}Ar,5n)^{215}U [57]. Evaporation residues recoiled from the target were separated in flight from the primary beam by the gas-filled recoil separator SHANS [58] and subsequently identified on the basis of energy –position –time correlation measurement. The α-particle energy and half-life of ^{215}U were determined to be 8.428(30) MeV and $0.73^{+1.33}_{-0.29}$ ms, respectively. In 2016, Zhang *et al.* identified two α-decaying states in ^{216}U, one for the ground state and the other for the isomeric state with $8^+(\pi h_{9/2}\pi_{7/2})$ configuration. The α-decay properties for ^{215,216}U and the systematics of 8^+ isomeric state in $N = 124, 126$ isotones were also investigated [59, 60]. In 2021, a new α-emitting isotope ^{214}U, produced by the fusion–evaporation reaction ^{182}W(^{36}Ar, 4n)^{214}U was identified by employing the gas-filled recoil separator SHANS and the recoil-α correlation technique. More precise α-decay properties of even –even nuclei ^{216,218}U were also measured in the reactions of ^{40}Ar and ^{40}Ca beams with ^{180,182,184}W targets [61].

In addition, taking into account the electrostatic screening effect caused by the superposition of the involved charges, Budaca *et al.* recently proposed a simple analytical model based on the Wentzel –Kramers – Brillouin (WKB) approximation to systematically study the half-lives of proton radioactivity [62]. The results show that with the increase of proton number Z, the difference between the outer turning point radii increases, corresponding to whether the electrostatic screening effect is included in the Coulomb barrier or not. Because the penetration probability is very sensitive to outer turning point radii, it is necessary to introduce the screened electrostatic barrier, i.e. Hulthen potential [63], in the process of dealing with the decay problem. In recent years, the Hulthen potential has been widely used to study the half-lives of α decay, proton radioactivity and two-proton radioactivity [64–66], and the calculated results reproduce the experimental data well.

In 2005, Tavares *et al.* first evaluated the α-decay half-lives of bismuth isotopes with angular momentum

l=5 carried away by the emitted α particle, based on the Gamow model [67]. Since then, it has been successfully generalized to calculate the α-decay half-lives of platinum isotopes with l=0 [68] and neptunium isotopes with l=0 and l=1 [69]. The calculations of these works are in good agreement with experimental data. Based on this model, considering the screened electrostatic barrier, in this work we systematically calculate the α-decay half-lives of uranium isotopes and explore the robustness of $N = 126$ shell closure at $Z = 92$ with the experimental data taken from the latest evaluated nuclear properties table NUBASE2020 [70].

This article is organized as follows. In Section II, the theoretical frameworks of the Gamow model and the screened electrostatic barrier are described in detail. The calculations and discussion are presented in Section III. Finally, Section IV gives a brief summary.

II. THEORETICAL FRAMEWORK

The α-decay half-life, an important indicator of nuclear stability, is calculated by

$$T_{1/2} = \frac{\ln 2}{\lambda},\qquad(1)$$

where the decay constant λ can be obtained by

$$\lambda = v_0 S_\alpha P_{se}.\qquad(2)$$

Here the frequency factor v_0, which represents the number of assaults on the barrier per unit of time [71, 72], is usually estimated as

$$v_0 = \frac{v}{2a} = \frac{1}{2a}\sqrt{\frac{2Q_\alpha}{\mu}},\qquad(3)$$

where v is the velocity of the α particle inside the parent nucleus. S_α is the spectroscopic factor (also known as α particle preformation probability at the nuclear surface) and P_{se} is the penetrability factor through the external barrier region [73]. They can be expressed as

$$S_\alpha = e^{-G_{ov}}, G_{ov} = \frac{2}{\hbar}\int_a^b \sqrt{2\mu[V(r)-Q_\alpha]}dr,$$
$$P_{se} = e^{-G_{se}}, G_{se} = \frac{2}{\hbar}\int_b^c \sqrt{2\mu[V(r)-Q_\alpha]}dr,\qquad(4)$$

where $\hbar$ is the reduced Planck constant, μ denotes the reduced mass of α particle and daughter nucleus in the center-of-mass coordinate with m_d and m_α being the mass of the daughter nucleus and α particle, and $V(r)$ is the total interaction potential between the emitted α particle and

daughter nucleus which is depicted in Fig. 1.

In general, $V(r)$ is composed of the nuclear potential $V_n(r)$, the Coulomb potential $V_c(r)$ and centrifugal potential $V_l(r)$ by default. It can be expressed as

$$V(r) = V_n(r) + V_c(r) + V_l(r). \quad (5)$$

Here, the Coulomb potential $V_c(r)$ is written as

$$V_c(r) = \frac{Z_\alpha Z_d e^2}{r}, \quad (6)$$

where Z_α and Z_d represent the proton numbers of α particle and daughter nucleus, respectively, and e^2 is the square of the electronic elementary charge. In the process of α decay, for the superposition of the involved charges, movement of the emitted particle which generates a magnetic field and the inhomogeneous charge distribution of the nucleus, the emitted α-daughter nucleus electrostatic potential behaves as a Coulomb potential at short distance and drops exponentially at large distance, i.e. the screened electrostatic effect [63–66]. This behaviour of electrostatic potential can be described as the Hulthen type potential which is defined as

$$V_h(r) = \frac{t Z_\alpha Z_d e^2}{e^{tr} - 1}, \quad (7)$$

where t is the screening parameter. The centrifugal potential $V_l(r)$ can be expressed as

$$V_l(r) = \frac{l(l+1)\hbar^2}{2\mu r^2}. \quad (8)$$

where l is the orbital angular momentum taken away by the emitted α particle. $l=0$ for the favored α decays, while $l \neq 0$ for the unfavored α decays. On the basis of conservation laws of angular momentum and parity, the minimum angular momentum $l_{\min}$ taken away by the α particle can be obtained by

$$l_{\min} = \begin{cases} \Delta_j, & \text{for even } \Delta_j \text{ and } \pi_p = \pi_d, \\ \Delta_j + 1, & \text{for even } \Delta_j \text{ and } \pi_p \neq \pi_d, \\ \Delta_j, & \text{for odd } \Delta_j \text{ and } \pi_p \neq \pi_d, \\ \Delta_j + 1, & \text{for odd } \Delta_j \text{ and } \pi_p = \pi_d, \end{cases} \quad (9)$$

where $\Delta_j = |j_p - j_d|$ with j_p, π_p, π_d, j_d being the spin and parity values of parent and daughter nuclei, respectively.

In addition, G_{ov} and G_{se} are the Gamow factors obtained by the integral from a to b in the overlapping barrier region and from b to c in the separation barrier region in Fig. 1. Here $b = R_d + R_\alpha$ is the separating radius, with R_d and R_α being the radii of the daughter nucleus and the
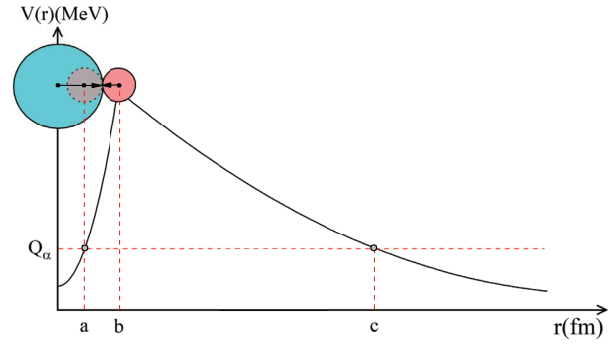

Fig. 1. (color online) Schematic diagram of one-dimensional α-daughter nucleus interaction potential potential $V(r)$. a, b and c are the three turning points of the potential energy while the barrier from a to b is the overlapping region and b to c is the separation region.

emitted α particle respectively. $a = R_p - R_\alpha$ and c are the inner and outer classical turning points of potential barrier, with R_p being the radius of the parent nucleus. The turning points satisfy the conditions $V(a) = V(c) = Q_\alpha$. The α-decay energy Q_α is calculated by

$$Q_\alpha = \Delta M_p - (\Delta M_d + \Delta M_\alpha) + 10^{-6}k(Z_p{}^\beta - Z_d{}^\beta) \text{ MeV}, \quad (10)$$

where ΔM_p, ΔM_d and ΔM_α represent the mass excess of parent nuclues, daughter nucleus and α particle, respectively, and the quantity kZ^β is the total binding energy of Z electrons in the atom, where $k = 8.7$ eV, $\beta=2.517$ for $Z \geq 60$ and $k=13.6$ eV, $\beta=2.408$ for $Z < 60$ [74]. Based on the above, the α-decay half-life can be expressed as

$$T_{1/2} = 1.0 \times 10^{-22} a \left(\frac{\mu}{Q_\alpha} \right)^{1/2} S_\alpha{}^{-1} P_{se}{}^{-1}. \quad (11)$$

In the overlapping region, since the α particle is still in the parent nucleus, the reduced mass μ can not be simply treated as a two-body problem. Duarte and Poenaru *et al.* have successfully dealt with this problem in α particle emitter ^{222}Rn by using $\mu(r) = [m_\alpha m_d/(m_\alpha + m_d)][(r-a)/(b-a)]^3$ and $V(r) = Q_\alpha + (V(b) - Q_\alpha)[(r-a)/(b-a)]^2$ [38, 75]. Encouraged by these two descriptions, the power functions of both $\mu(r)$ and $V(r)$ in the overlapping region can likewise be expressed by the following forms [67]

$$\mu(r) = \left(\frac{m_\alpha m_d}{m_\alpha + m_d} \right) \left(\frac{r-a}{b-a} \right)^p, \quad p \geq 0, \quad (12)$$

$$V(r) = Q_\alpha + (V(b) - Q_\alpha) \left(\frac{r-a}{b-a} \right)^q, \quad q \geq 1, \quad (13)$$

with

$$V(b) = V_h(b) + V_l(b) = \frac{tZ_\alpha Z_d e^2}{e^{tb} - 1} + \frac{l(l+1)\hbar^2}{2\mu b^2}. \tag{14}$$

Using Eqs. (4), (12) and (13), G_{ov} can be obtained as

$$G_{ov} = 0.4374702(b-a)\left(1 + \frac{p+q}{2}\right)^{-1}$$
$$\left\{\mu\left[\frac{2tZ_d e^2}{e^{tb} - 1} + \frac{20.9008l(l+1)}{\mu b^2} - Q_\alpha\right]\right\}^{1/2}, \tag{15}$$

where $\left(1 + \dfrac{p+q}{2}\right)^{-1}$ is defined as g with $0 \le g \le \dfrac{2}{3}$.

In the separation region, the parent nucleus has separated into two free individuals, the daughter nucleus and the α particle. We can deal with the reduced mass $\mu(r)$ as the reduced mass of the final decay system $\mu = m_\alpha m_d/(m_\alpha + m_d)$. Meanwhile, the potential energy $V(r)$ including the Hulthen type potential and centrifugal potential can be calculated by $V(r) = V_h(r) + V_l(r)$. From the above, G_{se} can be obtained as

$$G_{se} = 1.25988794Z_d\left(\frac{\mu}{Q_\alpha}\right)^{1/2} \times F, \tag{16}$$

where

$$F = \frac{x^{1/2}}{2y} \times \ln\left\{\frac{[x(x+2y-1)]^{1/2} + x + y}{(x/y)\left[1 + (1 + x/y^2)^{1/2}\right]^{-1} + y}\right\}$$
$$+ \arccos\left\{\frac{1}{2}\left[1 - \frac{1 - 1/y}{(1 + x/y^2)^{1/2}}\right]\right\}^{1/2}$$
$$- \left[\frac{1}{2y}(1 + x/2y - 1/2y)\right]^{1/2}, \tag{17}$$

with

$$x = \frac{20.9008l(l+1)}{\mu b^2 Q_\alpha}, \quad y = \frac{\ln\left(tZ_\alpha Z_d e^2/Q_\alpha + 1\right)}{2tb}. \tag{18}$$

III. RESULTS AND DISCUSSION

Based on the Gamow model, considering the screened electrostatic effect and introducing the Hulthen type potential, we propose an improved model to evaluate the α-decay half-lives of uranium isotopes. According to Eq. (9), we select as our database 14 nuclei with experimental α-decay half-lives of the ground-state to ground-state α transition with orbital angular momentum $l=0$, namely ^{216,218,221,222,224,226,228,229,230,232,233,234,236,238}U, excluding the newly synthesized nucleus ^{214}U, and 5 cases with $l=2$, namely ^{217,223,225,227,231}U. Based on this database, using a

genetic algorithm with an optimal solution of σ i.e. the deviation between the experimental data and calculated values as the objective function, we can obtain the values of the adjustable parameters t and g. In this work, σ is defined as follows

$$\sigma = \sqrt{\sum (\log_{10} T_{1/2}^{\text{calc}} - \log_{10} T_{1/2}^{\text{exp}})^2/n}, \tag{19}$$

where $\log_{10} T_{1/2}^{\text{exp}}$ and $\log_{10} T_{1/2}^{\text{calc}}$ are the logarithmic form of experimental and calculated α-decay half-lives respectively, and n is the number of nuclei involved for each case. The detailed results of the corresponding σ, t and g for the 14 α transitions with $l=0$ and the 5 with $l=2$ are listed in Table 1.

Using our improved Gamow model and the obtained values of parameters t and g, we calculate the α-decay half-lives for these uranium isotopes, 14 with $l=0$ and 5 with $l=2$. The detailed calculations are listed in Table 2. In this table, the first five columns denote the α transition, decay energy Q_α, spin−parity transformation, the minimum angular momentum taken away by the α particle, and the spectroscopic factor, respectively. The sixth column is the logarithm of the experimental α-decay half-life. The last five columns represent α-decay half-lives in logarithmic form of the uranium isotopes, calculated by our improved Gamow model, the modified Hatsukawa formula (XLZ) [52], the unified Royer formula (DZR) [51], the universal decay law (UDL) [42, 43] and the Viola−Seaborg−Sobiczewski formula (VSS) [48], respectively. As can be seen from this table, the calculated results of our model are close to the experimental values for most of the nuclei.

To intuitively display the accuracy of our results, in Fig. 2, we plot in logarithmic form the deviations between the experimental half-lives and the calculated values for α emitters of uranium isotopes with $l=0$ and $l=2$ using our improved Gamow model, XLZ, DZR, UDL and VSS. They are denoted as red sphere, gray square, blue pentagon, pink triangle and orange star, respectively. From this figure, we find that the differences for our improved Gamow model are basically concentrated near

Table 1. Standard deviations between the experimental α-decay half-lives and calculated values using our improved Gamow model for $l=0$ and $l=2$ uranium isotopes, along with the corresponding parameters t and g.

$\sigma/t/g$	l	
	$l = 0$	$l = 2$
cases	14	5
σ	0.141	0.340
t	5.5239×10^{-4}	3.0519×10^{-8}
g	0.0693	0.1549

Table 2. α-decay half-lives in logarithmic form of uranium isotopes calculated by our improved Gamow model, the modified Hatsukawa formula (XLZ), the unified Royer formula (DZR), the universal decay law (UDL) and the Viola–Seaborg–Sobiczewski formula (VSS), which are denoted as $\lg T_{1/2}^{\text{cal}}$, $\lg T_{1/2}^{\text{XLZ}}$, $\lg T_{1/2}^{\text{DZR}}$, $\lg T_{1/2}^{\text{UDL}}$ and $\lg T_{1/2}^{\text{VSS}}$, respectively. The experimental α-decay half-lives, spin and parity are taken from the latest evaluated nuclear properties table NUBASE2020 [70] except for ^{216}U and ^{218}U, whose accurate experimental α-decay half-lives are taken from [Phys. Rev. Lett. **126**, 152502 (2021)]. The Q_α values are taken from the latest evaluated atomic mass table AME2020 [76, 77]. The α-decay energies and half-lives are in units of MeV and s, respectively.

α transition	Q_α	$j_p^\pi \to j_d^\pi$	l	S_α	$\lg T_{1/2}^{\text{exp}}$	$\lg T_{1/2}^{\text{cal}}$	$\lg T_{1/2}^{\text{XLZ}}$	$\lg T_{1/2}^{\text{DZR}}$	$\lg T_{1/2}^{\text{UDL}}$	$\lg T_{1/2}^{\text{VSS}}$
Part I: α tansitions with l=0										
^{216}U→^{212}Th	8.37	$0^+ \to 0^+$	0	0.42	−2.65	−2.42	−2.35	−2.21	−2.18	−2.57
^{218}U→^{214}Th	8.61	$0^+ \to 0^+$	0	0.42	−3.19	−3.14	−3.07	−2.96	−2.91	−3.26
^{221}U→^{217}Th	9.93	$9/2^+\# \to 9/2^+\#$	0	0.43	−6.18	−6.49	−6.19	−6.12	−6.36	−5.70
^{222}U→^{218}Th	9.52	$0^+ \to 0^+$	0	0.43	−5.33	−5.56	−5.47	−5.50	−5.40	−5.63
^{224}U→^{220}Th	8.67	$0^+ \to 0^+$	0	0.42	−3.40	−3.39	−3.33	−3.24	−3.19	−3.42
^{226}U→^{222}Th	7.74	$0^+ \to 0^+$	0	0.41	−0.57	−0.58	−0.56	−0.36	−0.36	−0.61
^{228}U→^{224}Th	6.84	$0^+ \to 0^+$	0	0.41	2.75	2.72	2.72	2.99	2.94	2.66
^{229}U→^{225}Th	6.52	$3/2^+ \to 3/2^+$	0	0.40	4.24	4.07	4.26	4.71	4.28	4.89
^{230}U→^{226}Th	6.03	$0^+ \to 0^+$	0	0.40	6.24	6.31	6.30	6.61	6.50	6.19
^{232}U→^{228}Th	5.45	$0^+ \to 0^+$	0	0.39	9.34	9.39	9.36	9.68	9.51	9.19
^{233}U→^{229}Th	4.95	$5/2^+* \to 5/2^+*$	0	0.39	12.70	12.53	12.70	13.17	12.59	13.12
^{234}U→^{230}Th	4.90	$0^+ \to 0^+$	0	0.39	12.89	12.86	12.83	13.13	12.91	12.56
^{236}U→^{232}Th	4.61	$0^+ \to 0^+$	0	0.39	14.87	14.87	14.84	15.12	14.87	14.51
^{238}U→^{234}Th	4.31	$0^+ \to 0^+$	0	0.39	17.15	17.24	17.21	17.46	17.17	16.80
Part II: α tansition with l=2										
^{217}U→^{213}Th	8.47	$1/2^-\# \to 5/2^-$	2	0.12	−1.71	−1.81	−2.43	−1.84	−2.47	−1.95
^{223}U→^{219}Th	9.21	$7/2^+\# \to 9/2^+\#$	2	0.12	−4.19	−3.93	−4.53	−4.04	−4.63	−3.96
^{225}U→^{221}Th	8.05	$5/2^+ \to 7/2^+\#$	2	0.11	−1.21	−0.65	−1.33	−0.69	−1.34	−0.69
^{227}U→^{223}Th	7.28	$(3/2^+) \to (5/2)^+$	2	0.11	1.82	1.98	1.25	1.96	1.27	1.90
^{231}U→^{227}Th	5.62	$5/2^+\# \to (1/2^+)$	2	0.10	9.95	9.49	8.66	9.45	8.62	9.19
Part III: other α emitters in uranium isotopes										
^{219}U→^{215}Th	9.99	$9/2^+\# \to (1/2^-)$	5	−	−4.22	−	−6.29	−4.68	−6.47	−5.84
^{235}U→^{231}Th	4.72	$7/2^-* \to 5/2^+$	1	−	16.35	−	14.28	14.84	14.13	14.66
Part IV: Predictions										
^{214}U→^{210}Th	8.53	$0^+ \to 0^+$	0	0.42	−3.28	−2.85	−2.77	−2.64	−2.61	−3.04
^{215}U→^{211}Th	8.63	$5/2^-\# \to 5/2^-\#$	0	0.42	−	−3.13	−2.85	−2.58	−2.90	−2.41
^{220}U→^{216}Th	10.33	$0^+ \to 0^+$	0	0.43	−	−7.34	−7.23	−7.37	−7.24	−6.58
^{237}U→^{233}Th	4.27	$1/2^+ \to 1/2^+$	0	0.39	−	17.56	17.73	18.15	17.48	17.98
^{240}U→^{236}Th	4.08	$0^+ \to 0^+$	0	0.39	−	19.25	19.21	19.44	19.12	19.64
^{242}U→^{238}Th	3.71	$0^+ \to 0^+$	0	0.38	−	22.86	22.81	22.97	22.59	23.08
^{239}U→^{235}Th	4.17	$5/2^+ \to 1/2^+\#$	2	0.10	−	19.54	18.59	19.30	18.32	18.84
^{241}U→^{237}Th	3.86	$7/2^+\# \to 5/2^+\#$	2	0.10	−	22.42	21.44	22.11	21.08	21.58
^{243}U→^{239}Th	3.60	$9/2^-\# \to 7/2^+\#$	1	−	−	−	24.18	24.59	23.72	24.20

zero. This indicates that the calculated α-decay half-lives using our model can reproduce the experimental values well. It should be emphasized that the experimental α-decay half-lives are taken from the latest evaluated nuclear properties table NUBASE2020 [70] except for ^{216}U and ^{218}U, because the work [Phys. Rev. Lett. **126**, 152502 (2021)] in 2021 provides us with more accurate experimental data.
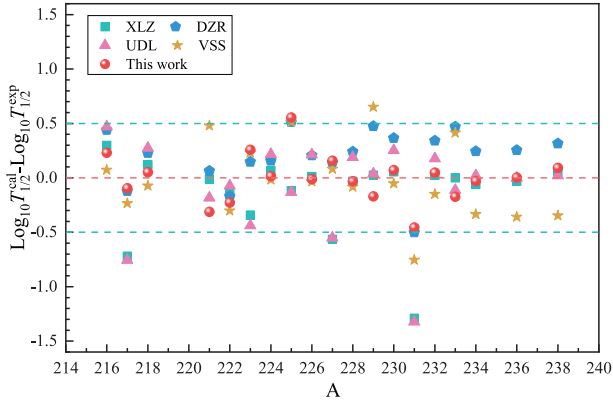
Fig. 2. (color online) Deviations in logarithmic form between the experimental and calculated α-decay half-lives for uranium isotopes with $l=0$ and $l=2$. The red sphere, gray square, blue pentagon, pink triangle and orange star represent the deviations calculated by our improved Gamow model, XLZ, DZR, UDL and VSS, respectively.

In the following, we extend the improved Gamow model to predict the α-decay half-lives of uranium isotopes with α transition $l=0$ and $l=2$ whose α decay is energetically allowed or observed but not yet quantified in NUBASE2020. The predicted α-decay half-lives are listed in Part IV of Table 2, along with the values calculated by XLZ, DZR, UDL and VSS for comparision.

The XLZ model was proposed by Xu *et al.* [52] to calculate the favored α-decay half-lives in 2022. It is expressed as

$$\log_{10}T_{1/2} = F(Z) \times \left(\frac{A_d}{A_p Q_\alpha}\right)^{1/2} \times \left[\arccos \sqrt{X} - \sqrt{X(1-X)}\right] - 20.446 + C(Z,N) + h, \quad (20)$$

where the coefficient $F(Z) = 28.274\sqrt{Z} + 2920.347/Z - 204.086$, and $C(Z,N)$ represents the effect of shells on α-decay half-lives. This can be written as

$$C(Z,N) = \begin{cases} 1.547 - 0.077(82-Z) - 0.050(126-N), \\ \quad 78 \le Z \le 82 \text{ and } 100 \le N < 126, \\ 1.397 - 0.116(Z-82) - 0.061(126-N), \\ \quad 82 < Z \le 90 \text{ and } 110 \le N \le 126. \end{cases} \quad (21)$$

The last term h represents the blocking effect of unpaired nucleons, whose values for different parent nuclei are expressed as

$$h = \begin{cases} 0, & \text{for even}-\text{even nuclei,} \\ h_p = h_n = 0.2018, & \text{for odd}-A \text{ nuclei,} \\ h_p + h_n = 0.4036, & \text{for odd}-\text{odd nuclei.} \end{cases} \quad (22)$$

The DZR model for α decay was proposed by Deng *et*

al. [51], and can be expressed as

$$\log_{10}T_{1/2} = a + bA^{1/6}\sqrt{Z} + c\frac{Z}{\sqrt{Q_\alpha}} + dl(l+1) + h, \quad (23)$$

where A, Z, Q_α and l represent the mass number, proton number, α decay energy of parent nuclei and the angular momentum taken away by the emitted α particle, respectively. By fitting the experimental data, the values of adjustable parameters are $a = -26.8125$, $b = -1.1255$, $c = -1.6057$, and $d = 0.0513$. The values of h for different α decay cases are expressed as

$$h_{\log} = \begin{cases} 0, & \text{for even-even nuclei,} \\ 0.2812, & \text{for odd } Z\text{-even } N \text{ nuclei,} \\ 0.3625, & \text{for even } Z\text{-odd } N \text{ nuclei,} \\ 0.7486, & \text{for odd-odd nuclei.} \end{cases} \quad (24)$$

The UDL model for α decay and cluster radioactivity modes was proposed by Qi *et al.* [42, 43], and can be expressed as

$$\log_{10}T_{1/2} = aZ_c Z_d \sqrt{\frac{A}{Q_c}} + b\sqrt{AZ_c Z_d(A_d^{1/3} + A_c^{1/3})} + c, \quad (25)$$

where $A = A_c A_d/(A_c + A_d)$, with A_c and A_d being the mass of cluster and daughter nucleus. The constants $a = 0.4314$, $b = -0.4087$ and $c = -25.7725$ are determined by fitting the experimental data of both α and cluster decays.

The VSS formula is a five-parameter formula put forward by Viola and Seaborg for calculating α-decay half-lives [41]. It can be expressed as

$$\log_{10}T_{1/2} = (aZ + B)Q_\alpha^{-1/2} + cZ + D + h_{\log}, \quad (26)$$

where Z is the atomic number of the parent nucleus and a, b, c and d are equal to 1.66175, −8.5166, −0.20228 and −33.9069, respectively [48]. The last term h_{log} is expressed as

$$h_{\log} = \begin{cases} 0, & \text{for even-even nuclei,} \\ 0.772, & \text{for odd } Z\text{-even } N \text{ nuclei,} \\ 1.066, & \text{for even } Z\text{-odd } N \text{ nuclei,} \\ 1.114, & \text{for doubly odd nuclei.} \end{cases} \quad (27)$$

For $l=0$, there are seven nuclei i.e. ^{214,215,220,237,240,242}U, among which ^{214}U was newly synthesized in 2021 and its measured α-decay half-life value is $0.52^{+0.95}_{-0.21}$ ms [61]. It can be well reproduced by the present model as 1.41 ms, which also checks the reliability of our improved Gamow model. Meanwhile, the pre-
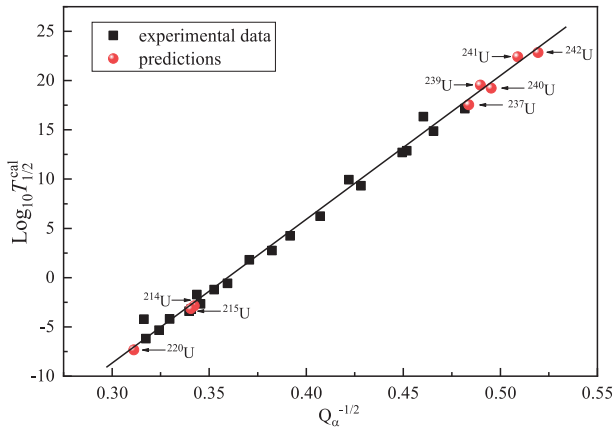
Fig. 3. (color online) Logarithmic form of α-decay half-life $\log_{10} T_{1/2}$ vs $Q_\alpha^{-1/2}$ for uranium isotopes. The line represents the Geiger–Nuttall law, black squares and red spheres denote the experimental and calculated half-lives, respectively.

Fig. 4. (color online) Relationship between the logarithmic form of α-decay half-lives $\log_{10} T_{1/2}$, α-decay energy Q_α, spectroscopic factor S_α and neutron number N of the parent nucleus : (a) for the logarithmic form of α-decay half-lives $\log_{10} T_{1/2}$, the red and blue triangle represent the experimental half-lives $T_{1/2}^{\exp}$ and predicted values $T_{1/2}^{\text{cal}}$, respectively; (b) for the α-decay energy Q_α; (c) for S_α with $l=0$ and $l=2$ in neptunium isotopes, where rhombus and pentagon represent $l=0$ and $l=2$ while pink and pale yellow denote experimental data and predicted values, respectively.

dicted α-decay half-lives of ^{215,220,237,240,242}U are 7.42×10^{-4}, 4.61×10^{-8}, 3.63×10^{17}, 1.77×10^{19} and 7.20×10^{22} s, respectively. For $l=2$, there are two nuclei, ^{239,241}U, with the predicted α-decay half-lives being 3.44×10^{19} and 2.64×10^{22} s. In order to test the reliability of predictions calculated by our model, we plot the relationship between $\log_{10} T_{1/2}$ and $Q_\alpha^{-1/2}$, i.e. the Geiger–Nuttall law [78], in Fig. 3. From this figure, we can clearly see that our predicted α-decay half-lives for these eight nuclei ^{214,215,220,237,239,240,241,242}U fit the linear relationship well. This indicates that our predicted results may be useful for future study of α-decay half-lives in newly synthesized uranium isotopes. In addition, there are two other α emitters of uranium isotopes ^{219}U and ^{235}U with $l=5$ and $l=1$ which can not be calculated by this work. We list them in Part III of Table 1.

To verify whether the shell closure $N=126$ is robust or not at $Z=92$, in Fig. 4 we plot the logarithmic form of α-decay half-lives $\log_{10} T_{1/2}$ and α-decay energy Q_α against the neutron number N of the parent nuclei. From this figure, it can be clearly seen that $\log_{10} T_{1/2}$ and Q_α present completely opposite trends with the change of N. Particularly, when N is less than 126, $\log_{10} T_{1/2}$ generally shows a slow trend to fluctuate, and drops sharply after 126 until $N=128$. A similar phenomenon can be seen on Q_α, where the values of Q_α increase dramatically to $N=128$ when the neutron number is greater than 126. The above phenomena reflect strong shell effects at $N=126$.

Finally, we extract the spectroscopic factor S_α in two cases with $l=0$ and $l=2$, then plot them versus the neutron number N of the parent nuclei in Fig. 4. From this figure, we find a amazing phenomenon that the S_α values are basically the same for α transitions with the same orbital angular momentum l, with the extracted values $S_\alpha \approx 0.406$ for $l=0$ and $S_\alpha \approx 0.112$ for $l=2$. It shows that high angular momentum will hinder the spectroscopic
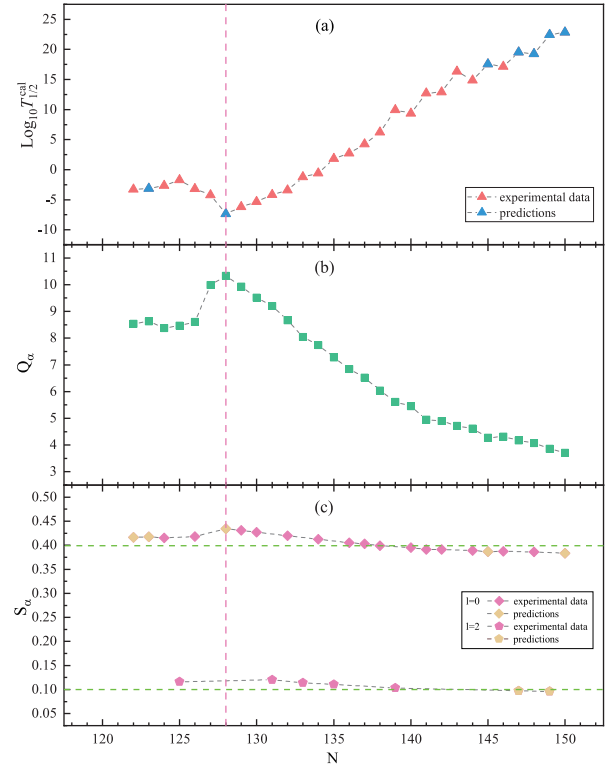
factor and α-decay half-life [79–81]. Meanwhile, its small variation trend can also reflect the robustness of $N=126$ at $Z=92$. The above phenomena are worthy of further study in the future.

IV. SUMMARY

In this work, based on the Gamow model, considering the effect of electrostatic screening, we systematically study the α-decay half-lives of uranium ($Z=92$) isotopes. The calculated results are in reasonable agreement with the experimental data. In addition, we extend this model to predict α-decay half-lives of uranium isotopes whose α decay is energetically allowed or observed but not yet quantified in NUBASE2020, along with the predictions of XLZ, DZR, UDL and VSS for comparision. The predicted results of our model and these three formulas are close and consistent in trend. In addition, the robustness of the shell closure $N=126$ is also verified at $Z=92$. Finally, we find the values of spectroscopic factor

S_α are basically the same for α transitions with the same orbital angular momentum l. The results of this work will prompt inquiries about nuclear structure and provide information for future experiments.

References

[1] S. Guo, X. Bao, Y. Gao *et al.*, Nucl. Phys. A **934**, 110 (2015)

[2] A. N. Andreyev, M. Huyse *et al.*, Phys. Rev. Lett **110**, 242502 (2013)

[3] H. F. Zhang and G. Royer, Phys. Rev. C **77**, 054318 (2008)

[4] A. N. Andreyev, M. Huyse *et al.*, Nature **405**, 430 (2000)

[5] M. Warda, J. L. Egido, and L.M. Robledo, Int. J. Mod. Phys. E **15**, 504 (2006)

[6] I. Muntian and A. Sobiczewski, Acta Phys. Pol. B **32**, 629 (2001)

[7] A. N. Andreyev, S. Antalic *et al.*, Phys. Rev. C **80**, 024302 (2009)

[8] E. Shin, Y. Lim, and Y. Oh, Phys. Rev. C **94**, 024320 (2016)

[9] R. Ernest and G. Hans, Proc. R. Soc. Lond. A **81**, 162 (1908)

[10] G. Gamow, Z. Phys. **51**, 204 (1928)

[11] R. W. Gurney and E. U. Condon, Nature **122**, 439 (1928)

[12] B. Buck, A. C. Merchant, and S. M. Perez, Phys. Rev. C **45**, 2247 (1992)

[13] B. Buck, A. C. Merchant, and S. M. Perez, Phys. Rev. Lett. **72**, 1326 (1994)

[14] C. Xu and Z. Z. Ren, Phys. Rev. C **69**, 024614 (2004)

[15] C. Xu and Z. Z. Ren, Phys. Rev. C **73**, 041301(R) (2006)

[16] F. R. Xu and J. C. Pei, Phys. Lett. B **642**, 322 (2006)

[17] D. D. Ni and Z. Z. Ren, Phys. Rev. C **80**, 014314 (2009)

[18] D. D. Ni and Z. Z. Ren, Nucl. Phys. A **825**, 145 (2009)

[19] K. P. Santhosh, B. Priyanka, and M. S. Unnikrishnan, Nucl. Phys.A **889**, 29 (2012)

[20] E. Javadimanesh, H. Hassanabadi *et al.*, Chin. Phys. C **36**, 964 (2012)

[21] S. A. Gurvitz and G. Kalbermann, Phys. Rev. Lett. **59**, 262 (1987)

[22] S. A. Gurvitz, P. B. Semmes, W. Nazarewicz *et al.*, Phys. Rev. A **69**, 042705 (2004)

[23] X. D. Sun, J. G. Deng, D. Xiang *et al.*, Phys. Rev. C **95**, 044303 (2017)

[24] X. D. Sun, C. Duan, J. G. Deng *et al.*, Phys. Rev. C **95**, 014319 (2017)

[25] X. D. Sun, P. Guo, and X. H. Li, Phys. Rev. C **93**, 034316 (2016)

[26] X. D. Sun, P. Guo, and X. H. Li, Phys. Rev. C **94**, 024338 (2016)

[27] X. D. Sun, X. J. Wu, B. Zheng *et al.*, Chin. Phys. C **41**, 014102 (2017)

[28] M. Bhattacharya and G. Gangopadhyay, Phys. Rev. C **77**, 047302 (2008)

[29] G. L. Zhang, X. Y. Le, and H. Q. Zhang, Nucl. Phys. A **823**, 16 (2009)

[30] D. N. Basu, Phys. Lett. B **566**, 90 (2003)

[31] P. R. Chowdhury, C. Samanta, and D. N. Basu, Phys. Rev. C **73**, 014612 (2006)

[32] C. Samanta, P. R. Chowdhury, and D. N. Basu, Nucl. Phys. A **789**, 142 (2007)

[33] P. R. Chowdhury, C. Samanta, and D. N. Basu, Phys. Rev. C **77**, 044603 (2008)

[34] K. Varga, R. G. Lovas, and R. J. Liotta, Phys. Rev. Lett. **69**, 37 (1992)

[35] H. F. Zhang, W. Zuo, J. Q. Li, and G. Royer, Phys. Rev. C **74**, 017304 (2006)

[36] H. F. Zhang and G. Royer, Phys. Rev. C **76**, 047304 (2007)

[37] J. M. Dong, H. F. Zhang, Y. Z. Wang *et al.*, Nucl. Phys. A **832**, 198 (2010)

[38] D. N. Poenaru, M. Ivascu, A. Sndulescu *et al.*, Phys. Rev. C **32**, 572 (1985)

[39] D. N. Poenaru, R. A. Gherghescu, and W. Greiner, Phys. Rev. Lett. **107**, 062503 (2011)

[40] D. N. Poenaru, R. A. Gherghescu, and W. Greiner, Phys. Rev. C **85**, 034615 (2012)

[41] V. E. Viola and G. T. Seaborg, J. Inorg. Nucl. Chem. **28**, 741 (1966)

[42] C. Qi, F. R. Xu, R. J. Liotta *et al.*, Phys. Rev. Lett. **103**, 072501 (2009)

[43] C. Qi, F. R. Xu, R. J. Liotta *et al.*, Phys. Rev. C **80**, 044326 (2009)

[44] G. Royer, J. Phys. G: Nucl. Part. Phys. **26**, 1149 (2000)

[45] Y. Hatsukawa, H. Nakahara, and D. C. Hoffman, Phys. Rev. C **42**, 674 (1990)

[46] Y. B. Qian and Z. Z. Ren, Nucl. Phys. A **852**, 82 (2011)

[47] Y. B. Qian, Z. Z. Ren, and D. D. Ni, Nucl. Phys. A **866**, 1 (2011)

[48] A. Sobiczewski, Z. Patyk, and S. Cwiok, Phys. Lett. B **224**, 1 (1989)

[49] D. T. Akrawy and A. H. Ahmed, Phys. Rev. C **100**, 044618 (2019)

[50] A. Soylu, and C. Qi, Nucl. Phys. A **1013**, 12221 (2021)

[51] J. G. Deng, H. F. Zhang, and G. Royer, Phys. Rev. C **101**, 034307 (2020)

[52] Y. Y. Xu, H. M. Liu *et al.*, Eur. Phys. J. A **58**, 16 (2022)

[53] Y. B. Qian and Z. Z. Ren, Phys. Rev. C **85**, 027306 (2012)

[54] Y. T. Oganessian, Radiochim. Acta **99**, 429 (2011)

[55] H. Suzuki, T. Kubo, N. Fukuda *et al.*, Phys. Rev. C **96**, 034604 (2017)

[56] N. T. Brewer, V. K. Utyonkov, K. P. Rykaczewski *et al.*, Phys. Rev. C **98**, 024317 (2018)

[57] H. B. Yang, Z. Y. Zhang, J. G. Wang *et al.*, Eur. Phys. J. A **51**, 88 (2015)

[58] Z. Y. Zhang, L. Ma, Z. G. Gan *et al.*, Nucl. Instrum. Methods B **317**, 315 (2013)

[59] Z. Y. Zhang, Z. G. Gan, L. Ma *et al.*, Nucl. Phys. Rev. **33**, 2 (2016)

[60] L. Ma, Z. Y. Zhang, Z. G. Gan *et al.*, Phys. Rev. C **91**, 051302(R) (2015)

[61] Z. Y. Zhang, H. B. Yang, M. H. Huang *et al.*, Phys. Rev. Lett. **126**, 152502 (2021)

[62] R. Budaca and A. I. Budaca, Eur. Phys. J. A **53**, 160 (2017)

[63] L. Hulthen, Ark. Mat. Astron. Fys. A **28**, 52 (1942)

[64] R. Budaca, A. I. Budaca, Chin, Phys. C **44**, 124102 (2020)

[65] J. H. Cheng, J. L. Chen, J. G. Deng *et al*., Nucl. Phys. A **987**, 350 (2019)
[66] Y. T. Zou, X. Pan, X. H. Li *et al*., Chin, Phys. C **45**, 104102 (2021)
[67] O. A. P. Tavares, E. L. Medeiros, and M. L. Terranovait, J. Phys. G: Nucl. Part. Phys. **31**, 129 (2005)
[68] O. A. P. Tavares, M. L. Terranovait, and E. L. Medeiros, Nucl. Instrum. Meth. B **243**, 256 (2006)
[69] Y. T. Zou, X. Pan, H. M. Liu *et al*., Phys. Scr. **96**, 075301 (2021)
[70] F. Kondev, M. Wang, W. Huang *et al*., Chin. Phys. C **45**, 030001 (2021)
[71] Y. W. Zhao, S. Q. Guo, and H. F. Zhang, Chin. Phys. C **42**, 074103 (2018)
[72] H. F. Zhang, G. Royer, and J. Q. Li, Phys. Rev. C **84**, 027303 (2011)
[73] C. Qi, R. Liotta, and R. Wyss, Prog. Part. Nucl. Phys. **105**, 214 (2019)
[74] K. N. Huang, M. Aoyagi, M. H. Chen *et al*., At. Data. Nucl. Data Tables **18**, 243 (1976)
[75] S. B. Duarte and M. G. Gonçalves, Phys. Rev. C **53**, 2309 (1996)
[76] W. J. Huang, M. Wang, F. Kondev *et al*., Chin. Phys. C **45**, 030002 (2021)
[77] M. Wang, W. J. Huang, F. G. Kondev *et al*., Chin. Phys. C **45**, 030003 (2021)
[78] H. Geiger and J. M. Nuttall, Phil. Mag. **22**, 613 (1911)
[79] J. G. Deng and H. F. Zhang, Phys. Rev. C **102**, 044314 (2020)
[80] J. G. Deng and H. F. Zhang, Chin. Phys. C **45**, 024104 (2021)
[81] J. G. Deng and H. F. Zhang, Phys. Lett. B **816**, 136247 (2021)